Title
Fermi Surface Changes across the Néel Phase Boundary of NdB6

Journal
Physical Review Letters, 97(14)

ISSN
0031-9007

Authors
Goodrich, RG
Harrison, N
Fisk, Z

Publication Date
2006-10-06

DOI
10.1103/physrevlett.97.146404

Fermi Surface Changes across the Néel Phase Boundary of NdB_6

R. G. Goodrich,[1] N. Harrison,[2] and Z. Fisk[3]

[1]*Department of Physics and Astronomy, Louisiana State University, Baton Rouge, Louisiana 70801, USA*
[2]*National High Magnetic Field Laboratory, Los Alamos National Laboratory, MS E536, Los Alamos, New Mexico 87545, USA*
[3]*Department of Physics, University of California, Irvine, California 92697, USA*

(Received 14 June 2006; published 5 October 2006)

We report de Haas-van Alphen measurements in both the antiferromagetic and paramagnetic regimes of NdB_6, which are shown to be separated by a second order upper critical field for antiferromagnetic ordering of $H_c \approx 30$ T when the magnetic field is parallel to [001]. The Fermi surface changes across the transition provide an ideal example of a system in which the effect of a one-dimensional magnetic periodic potential on doubling the unit cell (as originally predicted by Slater [Phys. Rev. **82**, 538 (1951)]) can be tuned by varying only the magnetic field. The Fermi surface within the paramagnetic phase resembles that observed in other hexaborides such as LaB_6 but with additional exchange splitting effects and weak correlations.

DOI: 10.1103/PhysRevLett.97.146404 PACS numbers: 71.18.+y, 75.20.Hr, 75.30.Fv

It has long been postulated that the inequivalency of the atomic sites in a type I antiferromagnet introduces a periodic potential that doubles the unit cell, causing the electronic structure to be modified [1]. This principle underlies our understanding of spin-density wave (SDW) formation in metals such as chromium [2]. Owing to the large effective exchange interaction J_{eff} between ordered moments in conventional SDW systems, however—being typically of order the Fermi temperature [3]—a direct measure of the change in Fermi surface topology between antiferromagnetic (AFM) and paramagnetic (PM) regimes has remained inaccessible to laboratory magnetic fields. In this Letter, we show that certain f-electron antiferromagnets can provide an alternative route to exploring such Fermi surface changes. The Ruderman-Kittel-Kasuya-Yosida (RKKY) exchange interaction J_{RKKY} is considerably smaller than J_{eff} in SDW systems [4], enabling the f electrons to be polarized in the laboratory. We show that such a polarization in NdB_6 destroys antiferromagnetism by way of a second order phase transition at a critical field $\mu_0 H_c \approx 30$ T for $\mathbf{H} \parallel [100]$. The loss of the one-dimensional magnetic periodic potential leads to a predictable restoration of the ellisoidal Fermi surface sheets centered on the X point of the cubic Brillouin zone [5].

Among f-electron antiferromagnets, cubic NdB_6 with a Néel transition temperature of $T_N \approx 8.3$ K [6] (see Fig. 1) has ideal physical properties for exploring perturbative changes in the electronic structure caused by a magnetic periodic potential $V(\mathbf{Q})$. In contrast to those compounds containing rare earth and actinide elements near the ends of the series in which residual Kondo screening leads to a reduced moment [7–10], the Fermi surface reconstruction is clearly evident in NdB_6 [5,11,12]. $4f$-hybridization effects are sufficiently weak for the $4f$ electrons to remain localized once the paramagnetic regime is accessed beyond H_c [4]. These are important considerations in ensuring that the creation (or destruction) of the staggered moment is the only significant change in the electronic structure at H_c. If the modulation is one-dimensional and occurs by way of a second order phase transition, it then becomes directly equivalent to the creation (or destruction) of the staggered moment at a SDW phase transition.

Prior studies have shown the $4f^3$-electron multiplet of Nd to be split by the cubic crystal electric field of the surrounding B_6 octahedra into a lowest lying Γ_8 quartet and a nearest excited Γ_6 doublet at ≈ 278 K [13,14]. As with the Ce analogue CeB_6, the Γ_8 quartet possesses both magnetic dipolar and electric quadrupolar degrees of freedom. Unlike with CeB_6, however, only the former orders in NdB_6 at $H = 0$, yielding a simple type I antiferromagnet with ordering vector $\mathbf{Q} = (0, 0, \frac{1}{2})$. The unit cell within the antiferromagnetic phase is therefore simply related to that

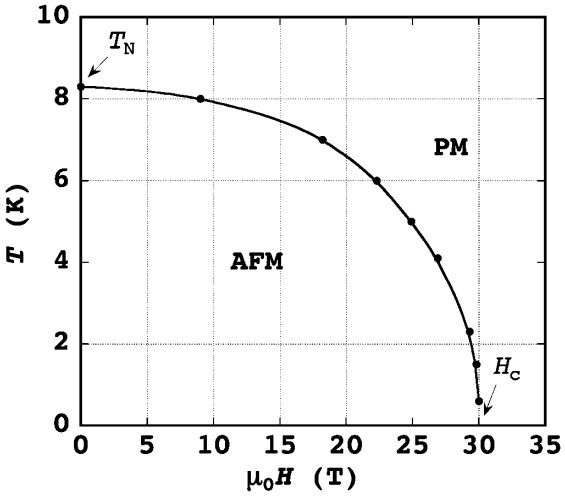

FIG. 1. H versus T phase diagram of NdB_6 for $\mathbf{H} \parallel [001]$ constructed from jumps in the differential susceptibility (induced voltage) observed in the magnetometer at several different temperatures. The line separating AFM and PM regions is drawn as a guide to the eye.

in the paramagnetic phase, leading to an equally simple modification of the Fermi surface topology [12]. Prior de Haas-van Alphen (dHvA) measurements have yielded a plethora of frequencies F that are significantly different than those observed in LaB_6 and other hexaboride compounds [5,11]. Low temperature magnetization measurements have also shown magnetic order to be destroyed at $\approx$24 T for $\mathbf{H} \parallel [110]$ and $\approx$21 T for $\mathbf{H} \parallel [111]$, with an intermediate phase appearing beyond $\approx$16 T in the latter case [15]. Until now, the paramagnetic regime has remained unexplored by means of the dHvA effect.

In the present experiments, Al-flux grown parallelepiped samples of $\approx 0.1 \times 0.2 \times 3$ mm^3 are measured in pulsed magnetic fields $\mathbf{H} \parallel [001]$ extending to $\approx$55 T using a magnetometer consisting of 450 turns of $\approx$10 μm copper wire wound on a $\approx$500 μm mandrel. The field-compensation coil is wound coaxially around it and connected to the preamplifier in series. Temperatures (T) between $\approx$450 mK and 10 K are stabilized using a plastic ^{3}He refrigerator. Figure 2 shows examples of the induced voltage $v \propto \partial M_z/\partial t$ in the magnetometer at $T \approx 600$ mK and $\approx$4 K plotted versus H.

The signal consists of dHvA oscillations between $\sim$10 and 55 T together with a jump in $v \propto \partial M_z/\partial t$ at H_c that is more clearly discernible at 4 K in Fig. 2. Such a jump is consistent with the change in slope of the differential susceptibility $\chi = \partial M_z/\partial H$ expected at a second order phase transition. Jumps observed at several different temperatures are then used to construct the phase diagram presented in Fig. 1. The observation of a single jump confirms the absence of a field-induced phase when $\mathbf{H} \parallel [100]$.

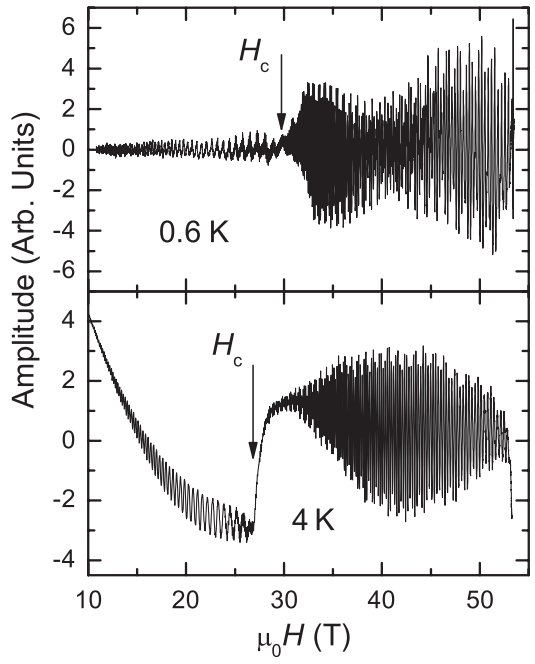

FIG. 2. Examples of the voltage induced in the magnetometer due to a sample of NdB_6 at $T \approx 0.6$ K and $\approx$ 4 K. H_c denotes the critical field for the given T.

Fourier transforms of the dHvA oscillations in the AFM and PM regimes are compared in Fig. 3. The spectral content within the AFM phase is similar to that obtained in prior studies [5,11]. The frequencies h, g, c, and a are further reproduced in the Fermi surface calculations of Kubo *et al.* [12]. Multiple combination frequencies also appear in the present study, particularly within the higher magnetic field region of the AFM phase, suggesting the possibility of magnetic interaction. The Fourier spectrum undergoes an abrupt change in Fig. 3 once the PM phase is reached (i.e., $\mu_0 H > 30$ T). The a frequency that dominates the signal for $25 < \mu_0 H < H_c$ is replaced by a new dominant but marginally different ($\sim$2% lower) frequency for $H > H_c$ that is almost identical to the α_3 frequency (to within $\sim$0.1%) observed in LaB_6 [5,7]. Frequencies very similar in value to the ϵ, γ, and $\alpha_{1,2}$ frequencies of LaB_6 [5,7] are also observed within the PM phase, indicating with certainty that $V(\mathbf{Q})$ has vanished. NdB_6 is therefore a

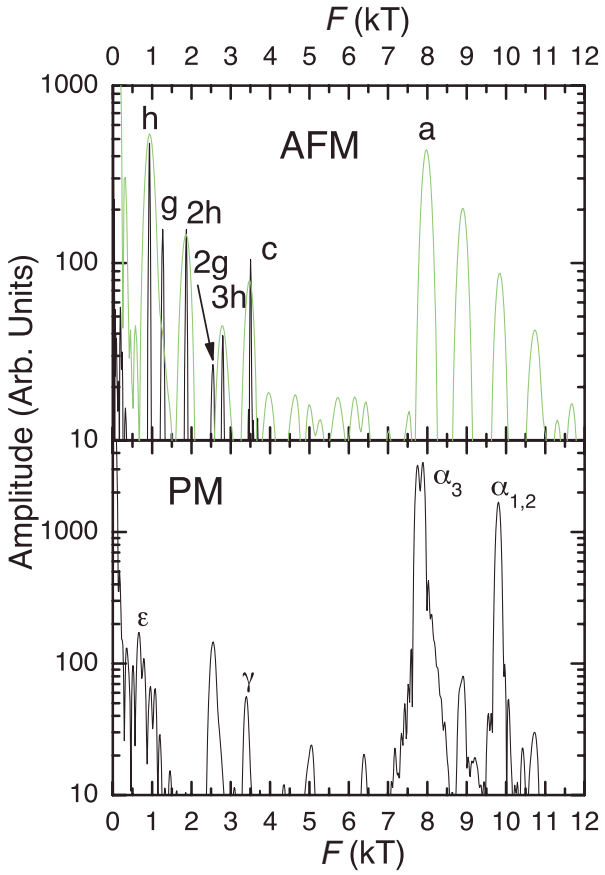

FIG. 3 (color online). Fourier transforms of the dHvA oscillations at $T \approx 600$ mK in both the AFM regime for $10 < \mu_0 H < 25$ T (black curve) and $25 < \mu_0 H < 30$ T (green or lighter curve) and also in the PM regime $32 < \mu_0 H < 52$ T. We have used a logarithmic scale and adopted the nomenclature introduced by Onuki *et al.* for labeling frequencies [11].

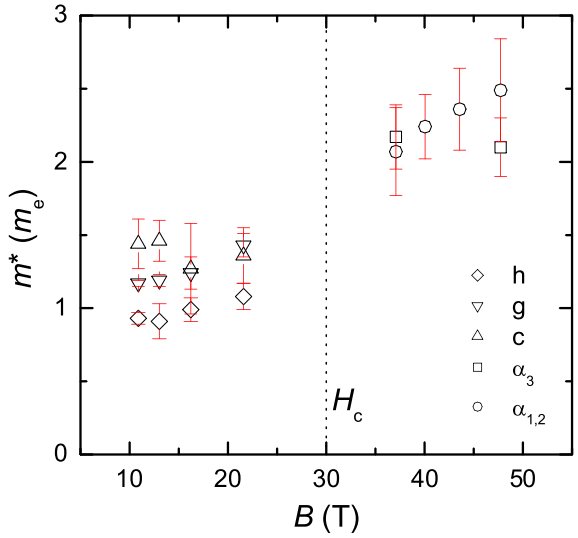

FIG. 4 (color online). Effective masses m^* estimated from the temperature dependence of the oscillation amplitudes of the principle dHvA frequencies in both the AFM and PM regions separated by H_c, extracted at different average values of the applied magnetic field H. The effective mass of the α_3 frequency becomes unobtainable for $40 \lesssim \mu_0 H \lesssim 45$ T due to a phase cancellation between spin-up and spin-down components of the dHvA effect.

particularly clear example of a material in which the electronic structure changes introduced by a magnetic periodic potential can be seen directly by tuning the applied magnetic field.

On extracting the effective masses m^* in Fig. 4 for each extremal orbit frequency from the temperature dependences of the oscillation amplitudes, values within the AFM phase are found to compare favorably with those measured by Onuki *et al.* [11]. Values of m^* for the $\alpha_{1,2,}$ and α_3 frequencies within the PM region are somewhat heavier than in the AFM phase [11] but similar to those observed in CeB_6 at high magnetic fields [16], suggesting that the degree of hybridization between the $4f$ electrons and the conduction electrons is similarly weak in both systems in strong magnetic fields. All estimates are approximately independent of field within the experimental error—the possible exception being the effective mass of the $\alpha_{1,2}$ orbit within the PM region, which displays a slight upward trend with field (we return to a discussion of this below).

Given that the Kondo effect is weak in NdB_6, direct exchange splitting is expected to have a more notable effect on the conduction electrons. Such a splitting can be seen directly on the higher harmonics of the α_3 frequency in Fig. 5, yielding clearly resolved separate spin-up and spin-down frequencies for harmonic indices greater than 3. The difference in dHvA frequency is $\Delta F \approx 87$ T at 40 T (or $\approx$1% of $F_{\alpha,3}$). As might be expected, the magnitude of the shift in each spin component is comparable

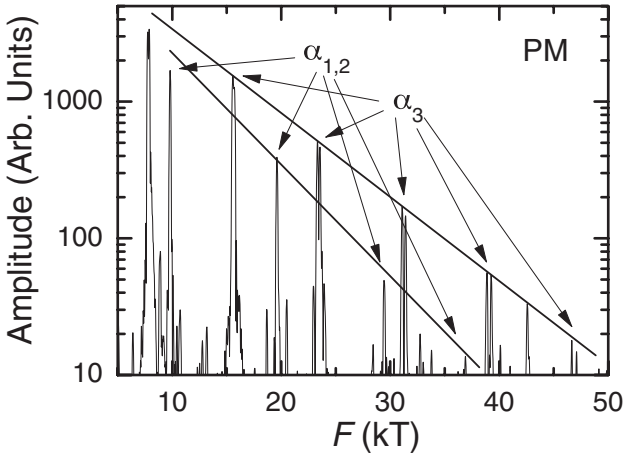

FIG. 5. Fourier transform of NdB_6 within the PM region over an expanded range of frequency on a logarithmic scale, yielding the $|H^{\mathrm{dir}}_{f-c}|$ exchange splitting of the α_3 dHvA frequency and its harmonics.

to the magnetic field scale of H_c. The direct exchange coupling H^{dir}_{f-c} can be estimated from the difference in effective Fermi energies $\varepsilon_F = \hbar e F/m^*$ between the two spin components, from which we obtain $|H^{\mathrm{dir}}_{f-c}| \approx \hbar e \Delta F/2m^* \approx 1.9$ meV. This value is smaller than that observed in PrB_6 [11] but larger than that observed in CeB_6 [17], although the dHvA effects are observed only within magnetically ordered phases in those systems. The splitting of the two spin components in NdB_6 causes each of their harmonics to decay in an almost ideal exponential fashion with increasing harmonic index in Fig. 5. A similar exponential decay of the $\alpha_{1,2}$ frequency in the absence of an observed splitting is, nevertheless, surprising. Such behavior is reminiscent of CeB_6 [18], where it was attributed to a strongly spin-dependent effective mass [19].

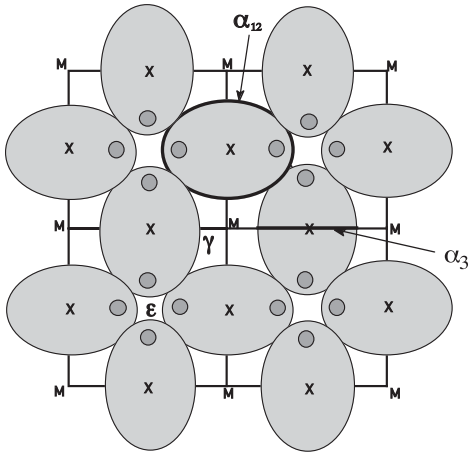

FIG. 6. Fermi surface of LaB_6 [7] within the ΓXM plane. The Fermi surface of NdB_6 is similar but with the added effect of exchange splitting.

Spin-dependent necks provide an explanation for the absence of a discernible splitting of the $\alpha_{1,2}$ frequency in NdB_6. In LaB_6 (as well as other hexaborides [7]), the large electron ellipsoids situated at the X point of the Brillouin zone barely touch each other within the ΓMX plane, giving rise to small necks that cause them to become interconnected as shown in Fig. 6. These necks lead to the creation of the holelike ϵ and γ orbits, but magnetic breakdown through them also enables the $\alpha_{1,2}$ frequency to continue to be observed, provided the necks do not become so large so as to completely diminish the tunneling probability. Exchange splitting (in addition to Zeeman splitting) can then cause the size of the necks to become different for each spin component. A particularly extreme case is that where the necks are large for one spin component but absent for the other. Such a scenario might explain both the absence of any discernible $\alpha_{1,2}$ splitting in Fig. 5 and the large relative amplitude of the $\alpha_{1,2}$ (at least for one spin component) compared to that in other hexaborides [7,11,18,20]. The large disparity between the dominant measured frequency $F_{\alpha 1,2} \approx 9.8$ kT and the value obtained from the difference $F'_{\alpha 1,2} = (F_{\mathrm{BZ}} - F_{\epsilon} - F_{\gamma})/2 \approx 10.0$ kT, where $F_{\mathrm{BZ}} \approx h/ea^2 \approx 24.0$ kT is the universal hexaboride Brillouin zone frequency [20], provides further evidence. Should H^{dir}_{f-c} couple the Nd moments antiparallel to the conduction electron spins [4], one conduction electron (spin-up) component would then become smaller, with a small or absent neck giving rise to the prominent measured frequency $F_{\alpha 1,2}$. The other (spin-down) component would become larger, with large necks inhibiting magnetic breakdown tunneling for that spin component, instead leading to the creation of prominent ϵ and γ Fourier amplitudes and a weak $F'_{\alpha 1,2}$ amplitude. A weak feature is indeed observed at $\approx$10.0 kT within the PM phase in Fig. 3. The difference $\Delta F \sim 200$ T between $F_{\alpha 1,2}$ and $F'_{\alpha 1,2}$ yields $|H^{\mathrm{dir}}_{f-c}| \approx 4$ meV—exceeding that estimated for the minimum cross section of the α ellipsoid by a factor of $\sim$2. Although the spin-up neck may be absent, the Zeeman term may eventually cause it to reappear in sufficiently strong magnetic fields $H \gg H_c$ at a Lifshitz 2.5 transition, providing another possible explanation for the upward trend in the $\alpha_{1,2}$ effective mass with field [21].

In summary, we report dHvA measurements in both the AFM and PM regimes of NdB_6, which are shown to be separated by a second order upper critical field for antiferromagnetic ordering of $H_c \approx 30$ T for $\mathbf{H} \parallel [001]$. The Fermi surface is observed to change radically but predictably across the transition, providing a clear example of a system in which the effect of a one-dimensional magnetic periodic potential on doubling the unit cell (as originally predicted by Slater [1]) can be tuned in a single compound by varying only the applied magnetic field. The Fermi surface within the paramagnetic phase resembles that observed in other hexaborides such as LaB_6 [7], albeit with exchange splitting present and weak correlations. NdB_6 therefore provides an essential localized f-electron precedent for understanding similar field-induced antiferromagnetism-to-paramagnetism transitions in more complex $4f$-electron systems where the $4f$-charge-degrees of freedom become involved [22,23].

This work was performed under the auspices of the National Science Foundation, the Department of Energy (U.S.), and the State of Florida. R. G. G. is supported directly by the NSF while Z. F. acknowledges Grant No. NSF-DMR-0503361. N. H. thanks Lev Gor'kov for useful comments.

[1] J. C. Slater, Phys. Rev. **82**, 538 (1951).
[2] E. Fawcett, Rev. Mod. Phys. **60**, 209 (1988).
[3] G. Grüner, Rev. Mod. Phys. **66**, 1 (1994).
[4] P. Fazekas, *Lecture Notes on Electron Correlation and Magnetism, Series in Modern Condensed Matter Physics* (World Scientific, Singapore, 1999), Vol. 5.
[5] A. P. J. van Deursen, Z. Fisk, and A. R. de Vroomen, Solid State Commun. **44**, 609 (1982).
[6] C. M. McCarthy and C. W. Tompson, J. Phys. Chem. Solids **41**, 1319 (1980).
[7] Y. Onuki *et al.*, J. Phys. Soc. Jpn. **58**, 3698 (1989).
[8] P. H. P. Reinders and M. Springford, J. Magn. Magn. Mater. **79**, 295 (1989).
[9] H. Shishido *et al.*, J. Phys. Soc. Jpn. **71**, 162 (2002).
[10] Y. Inada *et al.*, J. Phys. Soc. Jpn. **68**, 3643 (1999).
[11] Y. Onuki *et al.*. Phys. Rev. B **40**, 11 195 (1989).
[12] Y. Kubo *et al.*, J. Phys. Soc. Jpn. **62**, 205 (1993).
[13] M. Loewenhaupt and M. Prager, Z. Phys. B **62**, 195 (1986).
[14] G. Uimin and W. Brenig, Phys. Rev. B **61**, 60 (2000).
[15] S. Awaji *et al.*, J. Phys. Soc. Jpn. **68**, 2518 (1999).
[16] N. Harrison *et al.*, J. Phys. Condens. Matter **5**, 7435 (1993).
[17] T. Kasuya and H. Harima, J. Phys. Soc. Jpn. **65**, 1898 (1996).
[18] N. Harrison *et al.*, Phys. Rev. Lett. **81**, 870 (1998).
[19] R. G. Goodrich *et al.*, Phys. Rev. Lett. **82**, 3669 (1999).
[20] N. Harrison *et al.*, Phys. Rev. Lett. **80**, 4498 (1998).
[21] L. P. Gor'kov and P. D. Grigoriev, Phys. Rev. B **73**, 060401(R) (2006).
[22] P. Coleman *et al.*, J. Phys. Condens. Matter **13**, R723 (2001).
[23] J. Custers *et al.*, Nature (London) **424**, 524 (2003).